Biogeosciences, 17, 5079–5095, 2020
https://doi.org/10.5194/bg-17-5079-2020

Biogeosciences Open Access EGU

Identification of lower-order inositol phosphates (IP_5 and IP_4) in soil extracts as determined by hypobromite oxidation and solution ^{31}P NMR spectroscopy

Jolanda E. Reusser[1], René Verel[2], Daniel Zindel[2], Emmanuel Frossard[1], and Timothy I. McLaren[1]

[1]Department of Environmental Systems Science, ETH Zurich, Lindau, 8325, Switzerland
[2]Department of Chemistry and Applied Biosciences, ETH Zurich, Zurich, 8093, Switzerland

Correspondence: Jolanda E. Reusser (jolanda.reusser@usys.ethz.ch)

Received: 28 October 2019 – Discussion started: 28 November 2019
Revised: 20 August 2020 – Accepted: 26 August 2020 – Published: 21 October 2020

Abstract. Inositol phosphates (IPs) are a major pool of identifiable organic phosphorus (P) in soil. However, insight into their distribution and cycling in soil remains limited, particularly of lower-order IP (IP_5 and IP_4). This is because the quantification of lower-order IP typically requires a series of chemical extractions, including hypobromite oxidation to isolate IP, followed by chromatographic separation. Here, for the first time, we identify the chemical nature of organic P in four soil extracts following hypobromite oxidation using solution ^{31}P NMR spectroscopy and transverse relaxation (T_2) experiments. Soil samples analysed include A horizons from a Ferralsol (Colombia), a Cambisol and a Gleysol from Switzerland, and a Cambisol from Germany. Solution ^{31}P nuclear magnetic resonance (NMR) spectra of the phosphomonoester region in soil extracts following hypobromite oxidation revealed an increase in the number of sharp signals (up to 70) and an on average 2-fold decrease in the concentration of the broad signal compared to the untreated soil extracts. We identified the presence of four stereoisomers of IP_6, four stereoisomers of IP_5, and *scyllo*-IP_4. We also identified for the first time two isomers of *myo*-IP_5 in soil extracts: *myo*-(1,2,4,5,6)-IP_5 and *myo*-(1,3,4,5,6)-IP_5. Concentrations of total IP ranged from 1.4 to 159.3 mg P per kg soil across all soils, of which between 9 % and 50 % were comprised of lower-order IP. Furthermore, we found that the T_2 times, which are considered to be inversely related to the tumbling of a molecule in solution and hence its molecular size, were significantly shorter for the underlying broad signal compared to for the sharp signals (IP_6) in soil extracts following hypobromite oxidation. In summary, we demonstrate the presence of a plethora of organic P compounds in soil extracts, largely attributed to IPs of various orders, and provide new insight into the chemical stability of complex forms of organic P associated with soil organic matter.

1 Introduction

Inositol phosphates (IPs) are found widely in nature and are important for cellular functions in living organisms. They are found in eukaryotic cells where they operate in ion-regulation processes, as signalling or P storage compounds (Irvine and Schell, 2001). The basic structure of IP consists of a carbon ring (cyclohexanehexol) with one to six phosphorylated centres (IP_{1-6}) and up to nine stereoisomers (Angyal, 1963; Cosgrove and Irving, 1980). An important IP found in nature is *myo*-IP_6, which is used as a P storage compound in plant seeds. Another important species of IP is that of *myo*-(1,3,4,5,6)-IP_5, which is present in most eukaryotic cells at concentrations ranging from 15 to 50 µM (Riley et al., 2006). Species of IP_{1-3} are present in phospholipids such as phosphatidylinositol diphosphates and are an essential structural component of the cell membrane system (Strickland, 1973; Cosgrove and Irving, 1980).

Inositol phosphates have been reported to comprise more than 50 % of total organic phosphorus (P_{org}) in some soils (Cosgrove and Irving, 1980; McDowell and Stewart, 2006; Turner, 2007). Four stereoisomers of IP have been detected in soils, with the *myo* stereoisomer being the most abundant (56 %), followed by *scyllo* (33 %), *neo* and D-*chiro* (11 %;

Cosgrove and Irving, 1980; Turner et al., 2012). The largest input of *myo*-IP_6 to the soil occurs via the addition of plant seeds (Turner et al., 2002). However, the addition of *myo*-IP_6 to soil can also occur via manure input because monogastric animals are mostly incapable of digesting *myo*-IP_6 without the addition of phytases to their diets (Leytem et al., 2004; Leytem and Maguire, 2007; Turner et al., 2007b). An exception to this is pigs, which were found to at least partially digest phytate (Leytem et al., 2004), and transgenic pigs expressing salivary phytase (Golovan et al., 2001; Zhang et al., 2018). The accumulation of *myo*-IP_6 in soil occurs due to the negative charge of the deprotonated phosphate groups, which can coordinate on the charged surfaces of Fe- and Al-(hydro)-oxides (Anderson et al., 1974; Ognalaga et al., 1994), clay minerals (Goring and Bartholomew, 1951), and soil organic matter (SOM; McKercher and Anderson, 1989) or form insoluble precipitates with cations (Celi and Barberis, 2007). These processes lead to the stabilisation of IP in soil resulting in its accumulation and reduced bioavailability (Turner et al., 2002). In contrast, the sources and mechanisms controlling the flux of *scyllo*-, *neo*- and D-*chiro*-IP_6 in soil remain unknown but are thought to involve epimerisation of the *myo* stereoisomer (L'Annunziata, 1975).

Chromatographic separation of alkaline soil extracts revealed the presence of four stereoisomers of IP_6 and lower-order IP_{1-5} (Halstead and Anderson, 1970; Anderson and Malcolm, 1974; Cosgrove and Irving, 1980; Irving and Cosgrove, 1982). Irving and Cosgrove (1981) used hypobromite oxidation prior to chromatography to isolate the IP fraction in alkaline soils. The basis of this approach is that IPs are considered to be highly resistant to hypobromite oxidation, whereas other organic compounds (e.g. phospholipids and nucleic acids) will undergo oxidation (Dyer and Wrenshall, 1941; Turner and Richardson, 2004). The resistance of IP to hypobromite oxidation is thought to be due to the high charge density and steric hindrance, which is caused by the chair conformation of the molecule and the bound phosphate groups, with the P in its highest oxidation state. Hypobromite oxidation of inositol (without phosphate groups) mainly results in the formation of inososes, which have an intact carbon ring (Fatiadi, 1968). Fatiadi (1968) considered that the oxidation of bromine with inositol is stereospecific and comparable to catalytic or bacterial oxidants.

A limitation of chromatographic separation of alkaline extracts is that there is a mixture of unknown organic compounds that can co-elute with IP and result in an overestimation of IP concentrations (Irving and Cosgrove, 1981). However, this can also occur for IP, and historically, studies often reported the combined concentration of IP_6 and IP_5 due to a lack of differentiation in their elution times (McKercher and Anderson, 1968b). More recently, Almeida et al. (2018) investigated how cover crops might mobilise soil IP using hypobromite oxidation on sodium hydroxide–disodium ethylenediaminetetraacetic acid (NaOH-EDTA) extracts followed by chromatographic separation. The authors found that pools of *myo*-IP_6 and "unidentified IP" accounted for 30 % of the total extractable pool of P and hypothesised that the unidentified-IP pool consists solely of lower-order *myo*-IP. Pools of lower-order IP_{1-5} comprise on average 17 % of the total pool of IP in soil and account for an important pool of soil organic P in terrestrial ecosystems (Anderson and Malcolm, 1974; Cosgrove and Irving, 1980; Turner et al., 2002; Turner, 2007).

Since the 1980s, solution ^{31}P nuclear magnetic resonance (NMR) spectroscopy has been the most commonly used technique to characterise the chemical nature of organic P in soil extracts (Newman and Tate, 1980; Cade-Menun and Liu, 2014). An advantage of this technique is the simultaneous detection of all forms of organic P that come into solution, which is brought about by a single-step extraction with alkali and a chelating agent (Cade-Menun and Preston, 1996). However, a limitation of the technique has been the loss of information on the diversity and amount of soil IP compared to that typically obtained prior to 1980 (Smith and Clark, 1951; Anderson, 1955; Cosgrove, 1963). To date, solution ^{31}P NMR spectroscopy on soil extracts has only reported concentrations of *myo*-, *scyllo*-, *chiro*- and *neo*-IP_6. The fact that lower-order IPs were not reported in studies using NMR spectroscopy might be due to overlap of peaks in the phosphomonoester region, which makes peak assignment of specific compounds difficult (Doolette et al., 2009).

Turner et al. (2012) carried out hypobromite oxidation prior to solution ^{31}P NMR analysis of alkaline soil extracts to isolate the IP fraction. This had the advantage of reducing the number of NMR signals in the phosphomonoester region and consequently the overlap of peaks. The authors demonstrated the presence of *neo*- and *chiro*-IP_6 in NMR spectra via spiking of hypobromite oxidised extracts. Interestingly, the authors also reported the presence of NMR signals in the phosphomonoester region that could not be assigned to IP_6 and were resistant to hypobromite oxidation. They were not able to attribute the NMR signals to any specific P compounds but hypothesised based on their resistance to hypobromite oxidation that they were due to lower-order IP.

The aim of this study was to identify and quantify IP in soil extracts following hypobromite oxidation using solution ^{31}P NMR spectroscopy. In addition, the structural composition of phosphomonoesters in soil extracts following hypobromite oxidation was probed using solution ^{31}P NMR spectroscopy and transverse relaxation experiments. We hypothesise that a large portion of sharp peaks in the phosphomonoester region of untreated soil extracts are resistant to hypobromite oxidation, which would indicate the presence of a wide variety of IP. This would have major consequences on our understanding of P cycling in terrestrial (and aquatic) ecosystems, as many more organic P compounds and mechanisms would be involved than previously thought. Furthermore, a better understanding of these organic P compounds in soil would also help improve strategies to increase their biological utilisation, which may reduce the amount of fertiliser needed in

agricultural systems and thus influence the transfer of P to aquatic and marine ecosystems.

2 Experimental section

2.1 Soil collection and preparation

Soil samples were collected from the upper horizon of the profile at four diverse sites. These comprise a Ferralsol from Colombia, a Vertisol from Australia, a Cambisol from Germany, and a Gleysol from Switzerland (FAO and Group, 2014). The four soil samples were chosen from a larger collection based on their diverse concentration of P_{org} and composition of the phosphomonoester region in NMR spectra (Reusser et al., 2020). Background information and some chemical properties of the soils are reported in Table 1. Briefly, the Ferralsol was collected from an improved grassland in 1997 at the Carimagua Research Station's long-term Culticore field experiment in Columbia (Bühler et al., 2003). The Vertisol was collected from an arable field in 2018 located in southern Queensland. The site had been under native shrubland prior to 1992. The Cambisol was collected from a beech forest in 2014 and is part of the SPP 1685 – Ecosystem Nutrition project (Bünemann et al., 2016; Lang et al., 2017). The Gleysol was collected from the peaty top soil layer of a drained marshland in 2017, which has been under grassland for at least 20 years.

Soil samples were passed through a 5 mm sieve and dried at 60 °C for 5 d, except for the Ferralsol (sieved < 2 mm) and the Vertisol (ground < 2 mm), which were received dried. Total concentrations of C and N in soils were obtained using combustion of 50 mg of ground soil (to powder) weighed into tinfoil capsules (vario PYRO cube®, Elementar Analysensysteme GmbH). Soil pH was measured in H_2O with a soil-to-solution ratio of $1 : 2.5$ (w/w) using a glass electrode.

2.2 Soil phosphorus analyses

Total concentrations of soil P were obtained by X-ray fluorescence (XRF) spectroscopy (SPECTRO XEPOS ED-XRF, AMETEK®) using 4.0 g of soil sample ground to powder mixed with 0.9 g of wax (CEREOX Licowax, FLUXANA®). The XRF instrument was calibrated using commercially available reference soils. Concentrations of organic P for NMR analysis were obtained using the NaOH-EDTA extraction technique of Cade-Menun et al. (2002) at a soil-to-solution ratio of 1 : 10, i.e. extracting 4 g of soil with 40 mL of extractant.

2.3 Hypobromite oxidation

Hypobromite oxidation of NaOH-EDTA soil filtrates was carried out based on a modified version of the method described in Suzumura and Kamatani (1993) and Turner et al. (2012). The hypobromite oxidation procedure is similar to that reported in Turner (2020). Briefly, 10 mL of the NaOH-EDTA filtrate (Sect. 2.2) was placed in a three-necked round-bottom flask equipped with a septum, condenser, magnetic stir bar and thermometer (through a Claisen adapter with N_2 adapter). After the addition of 1 mL of 10 M aqueous NaOH and vigorous stirring, an aliquot of 0.6 mL Br_2 (which was cooled prior to use) was added, resulting in an exothermic reaction where some of the soil extracts nearly boiled. The optimal volume of Br_2 for oxidation was assessed in a previous pilot study using 0.2, 0.4, 0.6 and 0.8 mL Br_2 volumes and then observing differences in their NMR spectral features (Fig. S9). The reaction was heated to 100 °C within 10 min and kept at reflux for an additional 5 min. After cooling to room temperature, the solution was acidified with 2 mL of 6 M aqueous HCl solution in order to obtain a $pH < 3$, which was confirmed with a pH test strip. The acidified solution was reheated to 100 °C for 5 min under a stream of nitrogen to vaporise any excess bromine. The pH of the solution was gradually increased to 8.5 using 10 M aqueous NaOH solution. After dilution with 10 mL of H_2O, 5 mL of 50 % (w/w) ethanol and 10 mL of 10 % (w/w) barium acetate solution was added to the solution in order to precipitate any IP (Turner et al., 2012). The solution was then heated and boiled for 10 min and allowed to cool down overnight. The solution was subsequently transferred to a 50 mL centrifuge tube, and a 10 mL aliquot of 50 % (w/w) ethanol was added, manually shaken and centrifuged at 1500 g for 15 min. The supernatant was removed, and a 15 mL aliquot of 50 % (w/w) ethanol was added to the precipitate, shaken and then centrifuged again as before. The supernatant was removed and the process repeated once more to further purify the pool of IP. Afterwards, the precipitate was transferred with 20 mL of H_2O into a 100 mL beaker that contained a 20 mL volume (equating to a mass of 15 g) of Amberlite® IR-120 cation exchange resin beads in the H^+ form (Sigma-Aldrich, product no. 06428). The suspension was stirred for 15 min and then passed through a Whatman no. 42 filter paper. A 9 mL aliquot of the filtrate was frozen at −80 °C and then lyophilised prior to NMR analysis. This resulted in 18–26 mg of lyophilised material across all soils. Concentrations of total P in solutions were obtained using inductively coupled plasma optical emission spectrometry (ICP-OES). Concentrations of molybdate reactive P (MRP) were obtained using the malachite green method of Ohno and Zibilske (1991). The difference in concentrations of total P and MRP in solution is molybdate unreactive P (MUP), which is predominantly organic P for these samples. To assess the effect of hypobromite oxidation on the stability of an IP_6, duplicate samples of the Cambisol and the Gleysol were spiked with 0.1 mL of an 11 mM *myo*-IP_6 standard. The recovery of the added *myo*-IP_6 following hypobromite oxidation was calculated using Eq. (1):

$$\text{Spike recovery}\,(\%) = \frac{C_{\text{spiked}}\left(\frac{\text{mg}}{\text{L}}\right) - C_{\text{unspiked}}\left(\frac{\text{mg}}{\text{L}}\right)}{C_{\text{standard added}}\left(\frac{\text{mg}}{\text{L}}\right)}, \qquad (1)$$

Table 1. General characteristics of soil samples used in this study.

Soil type	Unit	Ferralsol	Vertisol	Cambisol	Gleysol
Country	–	Colombia	Australia	Germany	Switzerland
Coordinates sampling site	–	4°30′ N, 71°19′ W	27°52′ S, 151°37′ E	50°21′ N, 9°55′ E	47°05′ N, 8°06′ E
Elevation	m a.s.l.	150	402	800	612
Sampling depth	cm	0–20	0–15	0–7	0–10
Year of sampling	year	1997	2017	2014	2017
Land use	–	Pasture	Arable field	Forest	Pasture
C_{tot}	g C per kg soil	26.7	23.9	90.3	148.3
N_{tot}	g N per kg soil	1.7	1.9	6.6	10.9
pH in H_2O	–	3.6	6.1	3.6	5.0

where C_{spiked} and $C_{unspiked}$ are the concentrations of *myo*-IP_6 in NaOH-EDTA extracts following hypobromite oxidation of the spiked and unspiked samples, respectively. $C_{standard\ added}$ is the concentration of the added *myo*-IP_6 within the standard. As ^{31}P NMR spectroscopy of the standard revealed impurities, the concentration of *myo*-IP_6 in the standard was calculated based on the ^{31}P NMR spectrum.

2.4 Sample preparation for solution ^{31}P NMR spectroscopy

The lyophilised material of the untreated soil extracts was prepared for solution ^{31}P NMR spectroscopy based on a modification of the methods of Vincent et al. (2013) and Spain et al. (2018). Briefly, 120 mg of lyophilised material was taken and dissolved in 600 µL of 0.25 M NaOH–0.05 M Na_2 EDTA solution (ratio of 1 : 5). However, for the Cambisol sample, this ratio resulted in an NMR spectrum that exhibited significant line broadening. Therefore, this was repeated on a duplicate sample but at a smaller lyophilised-material-to-solution ratio (ratio of 1 : 7.5), as suggested in Cade-Menun and Liu (2014), which resolved the issue of poor spectral quality. The suspension was stored overnight to allow for complete hydrolysis of phospholipids and RNA (Doolette et al., 2009; Vestergren et al., 2012) and was then centrifuged at 10 621 g for 15 min. A 500 µL aliquot of the supernatant was taken, which was subsequently spiked with a 25 µL aliquot of a 0.03 M methylenediphosphonic acid (MDP) standard made in D_2O (Sigma-Aldrich, product no. M9508) and a 25 µL aliquot of sodium deuteroxide at 40 % (w/w) in D_2O (Sigma-Aldrich, product no. 372072). The solution was then mixed and transferred to a 5 mm diameter NMR tube.

A similar procedure was used for the soil extracts that had undergone hypobromite oxidation, except the total mass of lyophilised material (18–26 mg) was dissolved with 600 µL of a 0.25 M NaOH–0.05 M Na_2 EDTA solution. However, for the Cambisol sample, the NMR spectrum exhibited considerable line broadening, and an additional 400 µL aliquot of NaOH-EDTA solution was added to the NMR tube, mixed and then returned to the NMR spectrometer. This resolved the issue of poor spectral quality.

2.5 Solution ^{31}P NMR spectroscopy

Solution ^{31}P NMR analyses were carried out on all untreated and hypobromite oxidised soil extracts at the NMR facility of the Laboratory of Inorganic Chemistry (Hönggerberg, ETH Zurich). All spectra were obtained with a Bruker AVANCE III HD 500 MHz NMR spectrometer equipped with a cryogenic probe (CryoProbe™ Prodigy, Bruker Corporation, Billerica, MA). The ^{31}P frequency for this NMR spectrometer was 202.5 MHz, and gated broadband proton decoupling with a 90° pulse of 12 µs was applied. The spectral resolution under these conditions for ^{31}P was < 1 Hz. Longitudinal relaxation (T_1) times were determined for each sample with an inversion recovery experiment (Vold et al., 1968). This resulted in recycle delays ranging from 8.7 to 30.0 s for the untreated extracts and 7.8 to 38.0 s for the hypobromite oxidised soil extracts. The number of scans for the untreated extracts was set to 1024 or 4096, depending on the signal-to-noise ratio of the obtained spectrum. All hypobromite oxidised spectra were acquired with 3700 to 4096 scans.

2.6 Processing of NMR spectra

All NMR spectra were processed with Fourier transformation, phase correction and baseline adjustment within the TopSpin®software environment (version 3.5 pl 7, Bruker Corporation, Billerica, MA). Line broadening was set to 0.6 Hz. Quantification of NMR signals involved obtaining the integrals of the following regions: (1) up to four phosphonates (δ 19.8 to 16.4 ppm), (2) the added MDP (δ 17.0 to 15.8 ppm) including its two carbon satellite peaks, (3) the combined orthophosphate and phosphomonoester region (δ 6.0 to 3.0 ppm), (4) up to four phosphodiesters (δ 2.5 to -3.0 ppm), and (5) pyrophosphate (δ -4.8 to -5.4 ppm). Due to overlapping peaks in the orthophosphate and phosphomonoester region, spectral-deconvolution fitting (SDF) was applied as described in Reusser et al. (2020). In brief, the SDF procedure involved the fitting of an underlying broad

signal, based on the approach of Bünemann et al. (2008) and McLaren et al. (2019). We carried out the SDF with a non-linear optimisation algorithm in MATLAB® R2017a (The MathWorks, Inc.) and fitted visually identifiable peaks by constraining their linewidths at half height as well as the lower and upper boundary of the peak positions along with an underlying broad signal in the phosphomonoester region. The sharp signals of high intensity (e.g. orthophosphate) and the broad peak were fitted using Lorentzian line shapes, whereas sharp signals of low intensity were fitted using Gaussian line shapes. The NMR observability of total P (P_{tot}) in NaOH-EDTA extracts was calculated using Eq. (2) (Dougherty et al., 2005; Doolette et al., 2011b):

$$\text{NMR observability}\,(\%) = \frac{P_{\text{tot}}\ \text{NMR}}{P_{\text{tot}}\ \text{ICP-OES}} \times 100\,\%, \qquad (2)$$

where P_{tot} NMR refers to the total P content in milligrams of P per kilogram of soil detected in the soil extracts using solution ^{31}P NMR spectroscopy and P_{tot} ICP-OES refers to the total P concentration in milligrams of P per kilogram of soil measured in the soil extracts prior to freeze-drying using ICP-OES.

2.7 Spiking experiments

To identify the presence of IPs in hypobromite oxidised extracts, samples were spiked with a range of standards and then analysed again using NMR spectroscopy. This involved the addition of 5 to 20 µL aliquots of an IP standard solution directly into the NMR tube, which was then sealed with parafilm, manually shaken and then allowed to settle prior to NMR analysis. Each sample extract was consecutively spiked with no more than four IP standards. The NMR spectra of soil extracts after spiking were overlaid with the NMR spectra of unspiked soil extracts to identify the presence of IP across all soil samples. This comparison of NMR spectra was possible due to negligible changes in the chemical shifts of peaks among soil samples. The IP standards used in this study are listed in Table 2.

2.8 Transverse relaxation (T_2) experiments

Due to the presence of sharp and broad signals in the phosphomonoester region of NMR spectra on hypobromite oxidised soil extracts, transverse relaxation (T_2) experiments were carried out to probe their structural composition. The transverse relaxation (originally spin–spin relaxation) describes the loss of magnetisation in the x–y plane. This loss occurs due to magnetic-field differences in the sample, arising either by instrumentally caused magnetic-field inhomogeneities or by local magnetic fields in the sample caused by intramolecular and intermolecular interactions (Claridge, 2016). Generally, small, rapidly tumbling molecules exhibit longer T_2 relaxation times compared to large, slowly tumbling molecules (McLaren et al., 2019).

Briefly, solution ^{31}P NMR spectroscopy with a Carr–Purcell–Meiboom–Gill (CPMG) pulse sequence (Meiboom and Gill, 1958) was carried out on all hypobromite oxidised soil extracts, as described in McLaren et al. (2019). This involved a constant spin-echo delay (τ) of 5 ms, which was repeated for a total of eight iterations (spin-echo periods of 5, 50, 100, 150, 200, 250, 300 and 400 ms). A total of 4096 scans and a recycle delay of 4.75 s were used for all iterations. Transverse relaxation times for the aforementioned integral ranges were calculated using Eq. (3) within the TopSpin® software environment. Due to overlapping peaks in the orthophosphate and phosphomonoester region, spectral deconvolution was carried out to partition the NMR signal, as described in McLaren et al. (2019). The T_2 times of the partitioned NMR signals were calculated using Eq. (3) within RStudio© (version 1.1.442):

$$M\,(t) = M_0 \times e^{\left(-t \times T_2^{-1}\right)}, \qquad (3)$$

where M refers to the net magnetisation derived from the average angular momentum in the x–y plane, τ refers to the spin-echo delay in milliseconds (ms) and T_2 refers to the transverse relaxation time (ms).

2.9 Statistical analyses and graphics

Statistical analyses were carried out using Microsoft® Excel 2016 and MATLAB R2017a (© The MathWorks, Inc.). Graphics were created with Microsoft® Excel 2016 and MATLAB R2017a (© The MathWorks, Inc.). Solution (1D) ^{31}P NMR spectra were normalised to the peak intensity of MDP (δ 16.46 ppm). Spectra from the T_2 experiments were normalised to the peak intensity of *scyllo*-IP_6 (δ 3.22 ppm).

A one-way ANOVA was carried out in MATLAB R2017a (© The MathWorks, Inc.) with a subsequent multicomparison of mean values using Tukey's honestly significant difference procedure based on the Studentised range distribution (Hochberg and Tamhane, 1987; Milliken and Johnson, 2009).

3 Results

3.1 Phosphorus concentrations in soil extracts

Concentrations of total soil P as determined by XRF ranged from 320 to 3841 mg P per kg soil across all soils (Table 3). Concentrations of total P as estimated by the NaOH-EDTA extraction technique ranged from 160 to 1850 mg P per kg soil, which comprised 28 % to 51 % of the total soil P as determined by XRF. Pools of organic P comprised 28 % to 72 % of the total P in NaOH-EDTA untreated soil extracts.

Concentrations of total P in NaOH-EDTA soil extracts following hypobromite oxidation ranged from 77 to 578 mg P per kg soil (Table 3), which accounted for 31 % to 48 % (on average 38 %) of the total P originally present in the extracts.

Table 2. Standard solutions used for the spiking experiment of the hypobromite oxidised soil extracts. All standards were dissolved in 0.25 M NaOH and 0.05 M Na_2 EDTA.

Standard	Product number	Company or origin	Concentration of standard in NaOH-EDTA ($mg\,mL^{-1}$)
myo-IP_6	P5681	Merck (Sigma-Aldrich)	8.10
L-*chiro*-IP_6	Collection of Max Tate		2.39
D-*chiro*-IP_6	CAY-9002341	Cayman Chemical	2.00
neo-IP_6	Collection of Dennis Cosgrove*		4.62
D-*myo*-(1,2,4,5,6)-IP_5	CAY-10008452-1	Cayman Chemical	2.00
myo-(1,2,3,4,6)-IP_5	93987	Merck (Sigma-Aldrich)	2.00
D-*myo*-(1,3,4,5,6)-IP_5	CAY-10009851-1	Cayman Chemical	2.00
D-*myo*-(1,2,3,5,6)-IP_5	CAY-10008453-1	Cayman Chemical	2.00
scyllo-IP_5	Collection of Dennis Cosgrove		2.64
L-*chiro*-IP_5	Collection of Dennis Cosgrove		2.24
neo-IP_5	Collection of Dennis Cosgrove		2.45
myo-IP_4	Collection of Dennis Cosgrove		2.76
scyllo-IP_4	Collection of Dennis Cosgrove		2.41
neo-IP_4	Collection of Dennis Cosgrove		2.33

* Made up in 15 mM HCl.

Similarly, pools of organic P in NaOH-EDTA extracts following hypobromite oxidation were lower, comprising 22 % to 48 % (on average 36 %) of that originally present in untreated NaOH-EDTA extracts across all soils.

3.2 Solution ^{31}P NMR spectra of hypobromite oxidised soil extracts

The most prominent signal in the NMR spectra of untreated NaOH-EDTA soil extracts was that of orthophosphate at δ 5.25 ($\pm$0.25) ppm, followed by the phosphomonoester region ranging from δ 6.0 to 3.0 ppm (Fig. 1). There were also some minor signals due to pyrophosphate δ -5.06 ($\pm$0.19) ppm (all soils); phosphodiesters ranging from δ 2.5 to -2.4 ppm (not detected in the Vertisol); and phosphonates (not including the added MDP) at δ 19.8, 19.2 and 18.3 ppm (not detected in the Gleysol). However, these compounds comprised less than 8 % of the total NMR signal.

Following hypobromite oxidation of NaOH-EDTA extracts, the most prominent NMR signals were found in the orthophosphate (65 % of total NMR signal) and phosphomonoester (35 % of total NMR signal) region across all soils (Fig. 1). Phosphodiesters and pyrophosphates were removed following hypobromite oxidation in the Ferralsol, the Vertisol and the Cambisol (Germany). However, some signal remained in the Gleysol at low concentrations (0.4 % of the total NMR signal). Phosphonates were removed following hypobromite oxidation in the Ferralsol and the Vertisol, but a total of five sharp peaks in the phosphonate region were detected (δ 19.59, 18.58, 17.27 and 9.25 ppm) in the Cambisol. These peaks comprised 0.6 % of the total NMR signal.

The phosphomonoester region of NMR spectra on untreated NaOH-EDTA extracts exhibited two main features: (1) the presence of a broad signal centred at around δ 4.1 ($\pm$0.1) ppm with an average linewidth at half height of 256.12 Hz and (2) the presence of between 19 and 34 sharp signals. This was similarly the case for hypobromite oxidised extracts, except there was a decrease in the intensity of the broad signal and a change in the distribution and intensity of sharp signals. For the Cambisol and Gleysol, the number of sharp signals in the phosphomonoester region approximately doubled (to 40 and 70 sharp signals, respectively) following hypobromite oxidation. In contrast, less than half of the sharp signals remained in the Ferralsol following hypobromite oxidation (i.e. 14 of the 30 peaks originally present in the untreated extract), whereas one peak was removed following hypobromite oxidation in the Vertisol. There was little change (0.23 ppm) in the chemical shifts of peaks between the untreated and hypobromite oxidised extracts.

3.3 Identification and quantification of inositol phosphates (IP_6, IP_5 and IP_4) in soil extracts

Detailed views of the phosphomonoester regions of spiked samples are shown in Figs. S1 to S5 in the Supplement. The number of identified sharp peaks in the phosphomonoester region ranged from 7 (Vertisol) to 33 (Gleysol). *myo*- and *scyllo*-IP_6 were identified in the hypobromite oxidised extracts of all soils (Table 5). On average, 72 % of *myo*-IP_6 and 56 % of *scyllo*-IP_6 present in the untreated extracts remained in the hypobromite oxidised extracts (Table S1 in the Supplement). *neo*-IP_6 was identified in the 2-equatorial–4-axial

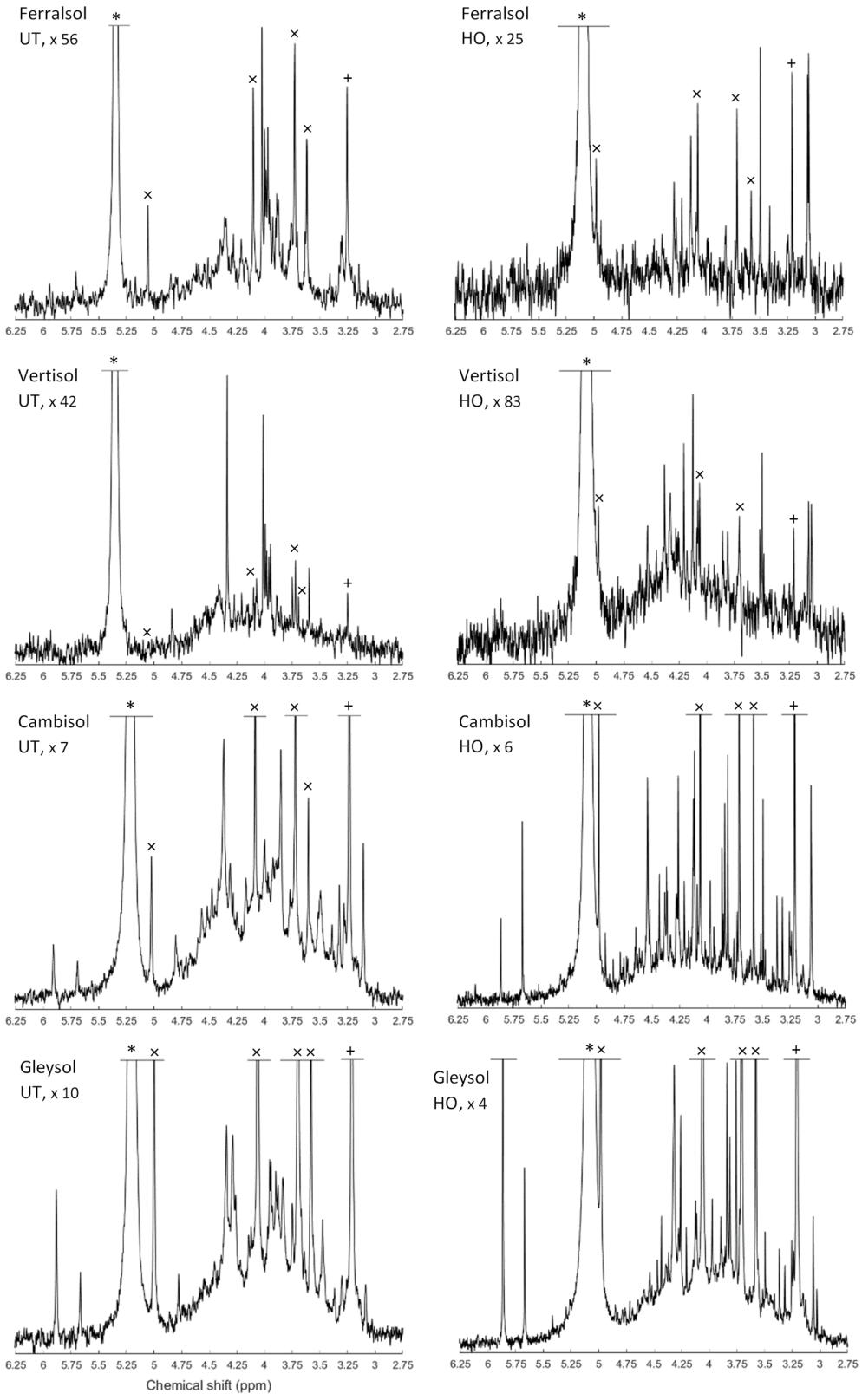

Figure 1. Solution ^{31}P nuclear magnetic resonance (NMR) spectra (500 MHz) of the orthophosphate and phosphomonoester region on untreated (UT) and hypobromite oxidised (HO) 0.25 M NaOH + 0.05 M EDTA soil extracts (Ferralsol, Vertisol, Cambisol and Gleysol). Signal intensities were normalised to the MDP peak intensity. The vertical axes were increased for improved visibility of spectral features, as indicated by a factor. The orthophosphate peak is marked with an asterisk. The symbol "×" marks the four individual peaks of *myo*-IP_6 and "+" the peak of *scyllo*-IP_6.

Table 3. Concentrations of total P as measured by XRF and 0.25 M NaOH + 0.05 M EDTA extractable P before and after hypobromite oxidation of soil extracts. Concentrations of total P in NaOH-EDTA extracts were determined by ICP-OES, whereas the concentration of molybdate reactive P (MRP) was determined by the malachite green method of Ohno and Zibilske (1991). Concentrations of molybdate unreactive P (MUP) were calculated as the difference between total P and MRP.

Measure		Ferralsol	Vertisol	Cambisol	Gleysol
XRF	P_{tot} (mg P per kg soil)	320	1726	3841	2913
NaOH-EDTA extractable P (untreated)	P_{tot} (mg P per kg soil)	160	484	1850	1490
	MRP (mg P per kg soil)	67	351	525	610
	MUP (P_{org}; mg P per kg soil)	93	133	1326	880
NaOH-EDTA extractable P (hypobromite oxidised)	P_{tot} (mg P per kg soil)	77	158	580	578
	MRP (mg P per kg soil)	32	111	283	231
	MUP (P_{org}; mg P per kg soil)	45	47	297	348

Table 4. Concentrations (mg P per kg soil) of P compounds in solution ^{31}P NMR spectra of 0.25 M NaOH + 0.05 M EDTA soil extracts (Ferralsol, Vertisol, Cambisol and Gleysol) before and after hypobromite oxidation (HO). Quantification was based on spectral integration and deconvolution fitting. The proportion of P detected in hypobromite oxidised extracts compared to that in untreated extracts is provided in brackets.

Phosphorus class		Ferralsol	Vertisol	Cambisol	Gleysol
Phosphonates	before HO	1.0	2.6	14.5	–
	after HO	–	–	3.0 (21)	0.2
Orthophosphate	before HO	54.8	221.4	434.3	368.3
	after HO	32.0 (58)	116.6 (53)	329.3 (76)	243.4 (66)
Phosphomonoester	before HO	36.3	39.1	501.1	399.2
	after HO	12.7 (35)	24.2 (62)	210.3 (42)	292.1 (73)
Broad peak in phosphomonoester region	before HO	21.6	30.9	305.8	216.7
	after HO	8.3 (39)	19.3 (63)	99.2 (32)	108.4 (50)
Phosphodiester	before HO	5.1	–	28.2	26.9
	after HO	–	–	–	2.0 (8)
Pyrophosphate	before HO	1.9	1.8	12.9	23.9
	after HO	–	–	–	–

and 4-equatorial–2-axial conformations and *chiro*-IP_6 in the 2-equatorial–4-axial confirmation of the oxidised extracts in the Cambisol and Gleysol but was absent in the Ferralsol and the Vertisol (Figs. S4 and S5 in the Supplement).

The *myo*, *scyllo*, *chiro* and *neo* stereoisomers of IP_5 were identified in various hypobromite oxidised extracts (Table 5). Two isomers of *myo*-IP_5 were identified in some extracts, which included *myo*-(1,2,4,5,6)-IP_5 and *myo*-(1,3,4,5,6)-IP_5. In addition, *scyllo*-IP_4 was detected in all soils except that of the Vertisol. There was insufficient evidence for the presence of *myo*-IP_4 in these soil samples, as only one of the two peaks of this compound was present in the NMR spectra of untreated extracts. This could possibly be due to the partial dephosphorylation of *myo*-IP_4 during the hypobromite oxidation procedure. The reason for the reduced resistance of lower-order IPs to hypobromite oxidation compared to IP_{5+6} might be due to their reduced steric hindrance and charge density, as fewer phosphate groups are bound to the inositol ring.

Concentrations of total IP ranged from 1.4 to 159.3 mg P per kg soil across all soils, which comprised between 1 % (Vertisol) and 18 % (Gleysol) of the organic P in untreated NaOH-EDTA extracts (Table 3). Pools of IP_6 were the most abundant form of IP, which ranged from 0.9 to 144.8 mg P per kg soil across all soils (Table 5). The proportion of IP_6 stereoisomers across all soils was on the order of *myo* (61 %, SD = 12), *scyllo* (29 %, SD = 3), *chiro* (6 %, SD = 8) and *neo* (4 %, SD = 5). Similarly, the *myo* and *scyllo* stereoisomers were also the most predominant forms of IP_5 but comprised between 83 % (Cambisol) and 100 % (Ferralsol and Vertisol) of total IP_5 (Table 5). Trace amounts of *scyllo*-IP_4 were also detected in three of the four soils. The ratio of total IP_6 to IP_5 differed across all soils (Fig. 2).

Table 5. Concentrations of identified inositol phosphates (IPs) in hypobromite oxidised 0.25 M NaOH + 0.05 M EDTA soil extracts (Ferralsol, Vertisol, Cambisol and Gleysol). Concentrations were calculated from solution ^{31}P NMR spectra using spectral-deconvolution fitting including an underlying broad signal. When no concentration is given, the IP compound was not detected in the respective soil extract. Chemical-shift positions are based on the NMR spectrum of the Cambisol extract (Fig. S8 in the Supplement). Peak positions varied by up to +0.018 ppm (Gleysol). Conformation equatorial (eq) and axial (ax) according to Turner et al. (2012).

Phosphorus compound	Chemical shift (δ ppm)	Concentrations (mg P per kg soil)			
		Ferralsol	Vertisol	Cambisol	Gleysol
myo-IP_6	4.97, 4.06, 3.70, 3.57	1.1	0.6	26.3	85.0
scyllo-IP_6	3.20	0.4	0.3	15.6	41.1
neo-IP_6 4-eq–2-ax	5.86, 3.75	–	–	1.4	8.8
neo-IP_6 2-eq–4-ax	4.36, 4.11	–	–	4.0	1.3
D-*chiro*-IP_6 2-eq–4-ax	5.66, 4.25, 3.83	–	–	9.4	8.6
myo-(1,2,4,5,6)-IP_5	4.42, 3.97, 3.72, 3.36, 3.25	–	–	7.0	4.1
myo-(1,3,4,5,6)-IP_5	4.12, 3.60, 3.23	–	–	2.8	1.3
scyllo-IP_5	3.81, 3.31, 3.05	0.7	0.5	10.8	6.1
neo-IP_5	4.64, 4.27, 4.01, 3.87, 3.13	–	–	3.3	2.1
chiro-IP_5	4.61, 3.39	–	–	0.9	–
scyllo-(1,2,3,4)-IP_4	4.12, 3.25	0.8	–	4.3	1.0
Total IP		3.0	1.4	85.9	159.3

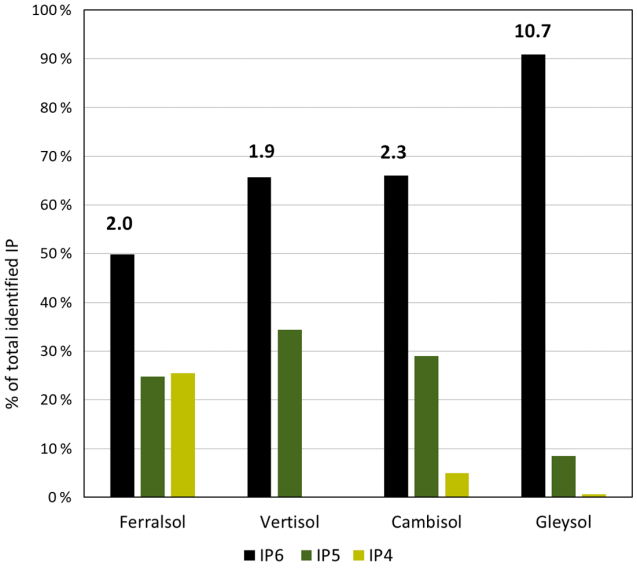

Figure 2. The proportion of total identifiable pools of inositol hexakisphosphates (IP_6), pentakisphosphates (IP_5) or tetrakisphosphates (IP_4) in the total pool of identifiable IP, as determined by solution ^{31}P NMR spectroscopy on four soil extracts (Ferralsol, Vertisol, Cambisol and Gleysol) following hypobromite oxidation. Values located above the IP_6 bar are the ratio of total identifiable IP_6 to total identifiable IP_5 in each soil sample.

If sharp peaks arising from IPs were identified in the NMR spectra on hypobromite oxidised extracts, a comparison was made with that of their corresponding untreated extracts. The sharp peaks of all stereoisomers of IP_6 were present in the untreated extracts. The five peaks of *myo*-(1,2,4,5,6)-IP_5 and the three peaks of *scyllo*-IP_5 were also identified. However, it was not possible to clearly identify other IP_5 compounds in untreated extracts due to overlapping signals. In the Gleysol, all three peaks of *scyllo*-IP_5 were detected, but only two of the possible five peaks could be clearly assigned to *myo*-(1,2,4,5,6)-IP_5. In the Ferralsol, both peaks of *scyllo*-IP_4 were present in the untreated extract, but only two of the three possible peaks could be assigned to *scyllo*-IP_5. In the Vertisol, no IP_5 was identified. Concentrations of IP in untreated extracts assessed by spectral-deconvolution fitting were generally double those measured in hypobromite oxidised extracts. Recoveries of added *myo*-IP_6 in the Gleysol and Cambisol following hypobromite oxidation were 47 % and 20 %, respectively.

3.4 Spin-echo analysis of selected P compounds

Due to the presence of sharp and broad signals in hypobromite oxidised soil extracts, the structural composition of phosphomonoesters was probed. A comparison of the NMR spectra at the lowest ($1^*\tau$) and highest ($80^*\tau$) pulse delays revealed a fast-decaying broad signal for all hypobromite oxidised soil extracts, which was particularly evident in the Gleysol (Fig. 3). Calculated T_2 times of all IP_6 stereoisomers were longer than those of the broad signal (Table 6). The T_2 times of *scyllo*-IP_6 (on average 175.8 ms, SD = 49.7) were generally the longest of all stereoisomers of IP_6. The T_2 time of the orthophosphate peak was the shortest, which was on average 11.5 ms (SD = 4.9).

The average ($n = 4$) T_2 time of the broad peak was significantly different than that of *scyllo*- and *myo*-IP_6 ($p < 0.05$). Significant differences in the T_2 times of *neo*- and D-*chiro*-

Table 6. Transversal relaxation times (T_2) of various P species in the orthophosphate and phosphomonoester regions as determined by solution ^{31}P nuclear magnetic resonance (NMR) spectroscopy and a Carr–Purcell–Meiboom–Gill (CPMG) pulse sequence on hypobromite oxidised soil extracts.

Phosphorus compound	T_2 (ms)			
	Ferralsol	Vertisol	Cambisol	Gleysol
myo-IP_6	163	140	139	121
scyllo-IP_6	250	155	154	144
neo-IP_6	–	–	203	102
D-chiro-IP_6	–	–	108	132
Orthophosphate	14	9	17	6
Broad peak	44	69	89	62

IP_6 were not tested, as these compounds were not detected in the Ferralsol and the Vertisol.

4 Discussion

4.1 Pools of phosphorus in untreated and hypobromite oxidised soil extracts

On average, 44 % of total P (as measured with XRF) was extracted by NaOH-EDTA, which is consistent with previous studies (Turner, 2008; Li et al., 2018; McLaren et al., 2019). The non-extractable pool of P is likely to comprise inorganic P as part of insoluble mineral phases but could also contain some organic P (McLaren et al., 2015a). Nevertheless, the NaOH-EDTA extraction technique is considered to be a measure of total organic P in soil, which can be subsequently characterised by solution ^{31}P NMR spectroscopy (Cade-Menun and Preston, 1996).

Hypobromite oxidation resulted in a decrease in the concentration of inorganic and organic P in NaOH-EDTA extracts across all soils. The decrease of organic P is consistent with previous studies (Turner and Richardson, 2004; Turner et al., 2012; Almeida et al., 2018). However, Almeida et al. (2018) reported an overall increase in the concentration of inorganic P following hypobromite oxidation, which the authors proposed to be caused by the degradation of organic P forms not resistant to hypobromite oxidation. A decrease in the concentration of organic P in NaOH-EDTA extracts following hypobromite oxidation was expected based on the oxidation of organic molecules containing P. The products of hypobromite oxidation are most probably carbon dioxide, simple organic acids from the oxidative cleavage of the phosphoesters and orthophosphate (Irving and Cosgrove, 1981; Sharma, 2013).

Overall, hypobromite oxidation of NaOH-EDTA soil extracts resulted in a considerable increase in the number of sharp peaks and a decrease in the broad underlying peak in the phosphomonoester region compared to untreated soil extracts. This was particularly the case for the Cambisol and the Gleysol, which had high concentrations of extractable organic P. Since the broad peak is thought to be closely associated with the SOM (Dougherty et al., 2007; Bünemann et al., 2008; McLaren et al., 2015b), its decrease in soil extracts following hypobromite oxidation is consistent with that observed for other organic compounds (Turner et al., 2012). Our results indicate that a majority of sharp peaks present in the phosphomonoester region of untreated soil extracts are stable to hypobromite oxidation and are therefore likely to be IPs.

Across all soils, 5 to 15 peaks in the phosphomonoester region were removed following hypobromite oxidation compared to those in untreated extracts, which are likely due to the oxidation of α- and β-glycerophosphate (Doolette et al., 2009; McLaren et al., 2015b), RNA mononucleotides (8 peaks; Vincent et al., 2013), glucose 6-phosphate, phosphocholine, glucose 1-phosphate, or phosphorylethanolamine (Cade-Menun, 2015).

4.2 Phosphorus assignments of sharp peaks in hypobromite oxidised extracts

The detection of *myo-, scyllo-*, *chiro* and *neo*-IP_6 in untreated and hypobromite oxidised soil extracts is consistent with previous studies using chromatography (Irving and Cosgrove, 1982; Almeida et al., 2018) and NMR (Turner and Richardson, 2004; Doolette et al., 2011a; Vincent et al., 2013; Jarosch et al., 2015; McLaren et al., 2015b). Turner et al. (2012) suggested that hypobromite oxidised extracts only contained *neo*-IP_6 in the 4-equatorial–2-axial conformation due to the absence of signals from the 2-equatorial–4-axial conformation. In the current study, both conformations could be identified in two of the four soil extracts, which is likely due to improved spectral resolution and sensitivity. The relative abundances of the four identified stereoisomers of IP_6 in soil extracts were similar to previous studies (Irving and Cosgrove, 1982; Turner et al., 2012).

Several studies have shown overlap of peaks relating to RNA mononucleotides and those of α- and β-glycerophosphate, which are the alkaline hydrolysis products of RNA and phospholipids, respectively. However, in the current study, several sharp peaks were present in hypobromite oxidised extracts which are in the chemical-shift range of RNA mononucleotides and α- and β-glycerophosphate. Whilst a peak at δ 4.36 ppm would be assigned to α-glycerophosphate based on spiking experiments in the untreated extracts of the Cambisol and the Gleysol, hypobromite oxidation revealed the presence of the 2-equatorial–4-axial C2,5 peak of *neo*-IP_6 at δ 4.37 ppm and also an unidentified peak at δ 4.36 ppm in the Cambisol. Therefore, the assignment and concentration of α-glycerophosphate may be unreliable in some soils of previous studies.

For the first time, we identified lower-order IP (IP_5 and IP_4) in soil extracts using solution ^{31}P NMR spectroscopy.

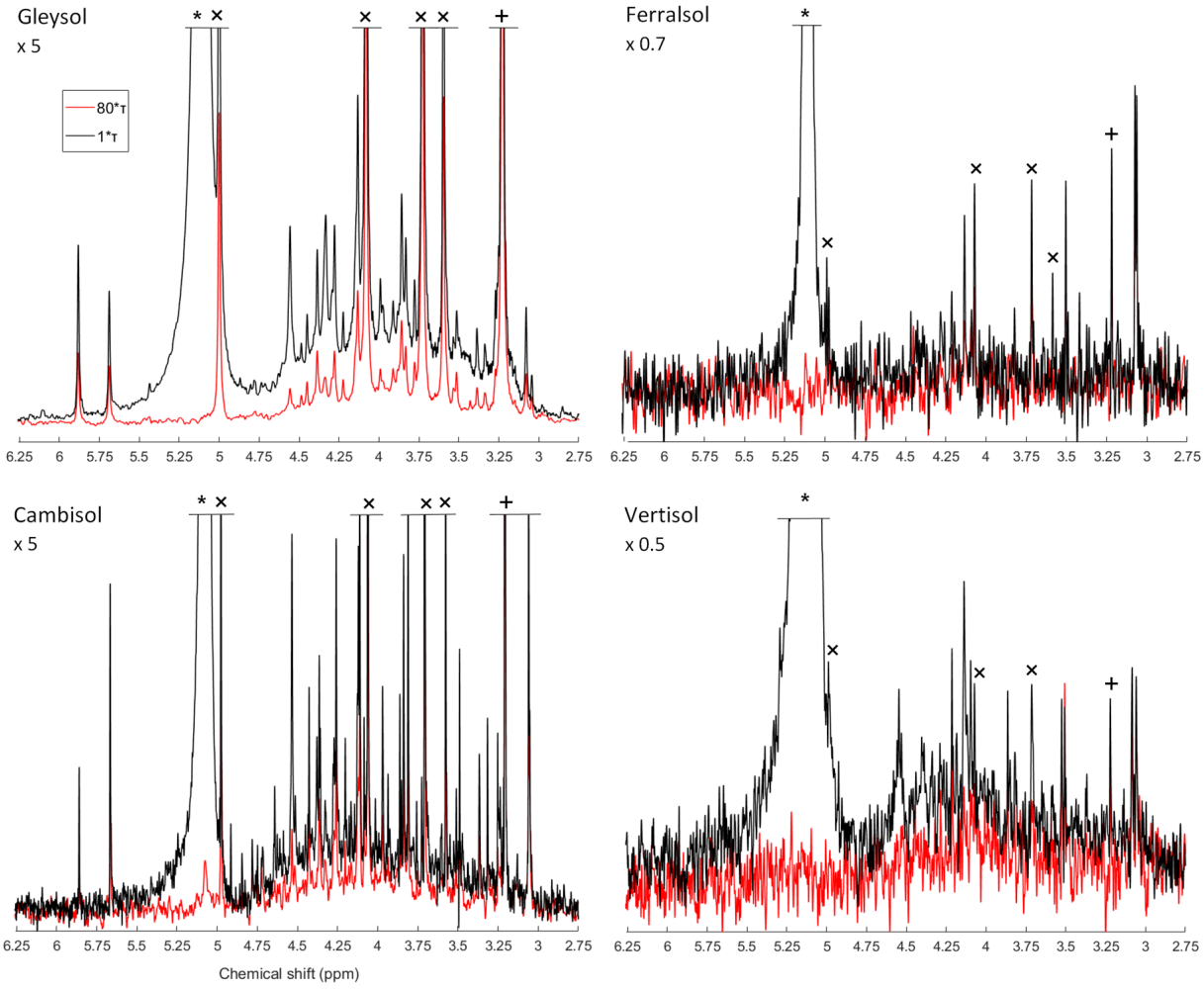

Figure 3. Solution ^{31}P NMR spectra of hypobromite oxidised soil extracts acquired with a CPMG pulse sequence with $1^{*}\tau$ (black) and $80^{*}\tau$ (red) spin-echo delays. The orthophosphate (*), *scyllo*-IP_6 (+) and *myo*-IP_6 peaks (×) are marked accordingly. Spectra were normalised to the maximum *scyllo*-IP_6 peak intensity in the $1^{*}\tau$ spectrum for each soil. The vertical axes were increased or decreased for better visualisation by an indicated factor.

Smith and Clark (1951) were the first to suggest the presence of IP_5 in soil extracts using anion-exchange chromatography, which was later confirmed (Anderson, 1955; Cosgrove, 1963; McKercher and Anderson, 1968b). Halstead and Anderson (1970) reported the presence of all four stereoisomers (*myo*, *scyllo*, *neo* and *chiro*) in the lower ester fractions (IP_2–IP_4) as well as in the higher ester fractions (IP_5, IP_6) isolated from soil, with the *myo* stereoisomer being the main form in all fractions. In the current study, all four stereoisomers of IP_5 could be detected in the hypobromite oxidised soil extracts, of which the *myo* and *scyllo* stereoisomers were the most abundant. The relative abundances of IP_5 stereoisomers are consistent with the findings of Irving and Cosgrove (1982) using gas-liquid chromatography on the combined $IP_6 + IP_5$ fraction. The detection of all four stereoisomers of IP_5 in NMR spectra provides direct spectroscopic evidence for their existence in soil extracts.

In addition to the four stereoisomers of IP_5, we were able to identify the presence of two isomers of *myo*-IP_5 in the Cambisol and Gleysol, i.e. *myo*-(1,2,4,5,6)-IP_5 and *myo*-(1,3,4,5,6)-IP_5. These two isomers have not yet been detected in soil extracts. A distinction of different *myo*-IP_5 isomers was not reported in earlier studies using chromatographic separation. In non-soil extracts, *myo*-(1,2,4,5,6)-IP_5 was detected by Doolette and Smernik (2016) in grapevine canes and *myo*-(1,3,4,5,6)-IP_5 as the thermal-decomposition product of a phytate standard (Doolette and Smernik, 2018). It is possible that an abiotic transformation of *myo*-IP_6 to *myo*-(1,3,4,5,6)-IP_5 occurs, which could then be adsorbed by soil constituents. Stephens and Irvine (1990) reported *myo*-(1,3,4,5,6)-IP_5 as an intermediate in the synthesis of IP_6 from *myo*-IP in the cellular slime mould *Dictyostelium*. Therefore, *myo*-(1,3,4,5,6)-IP_5 could have been biologically added to the soil. Furthermore, *myo*-(1,3,4,5,6)-IP_5 was present in dif-

ferent animal feeds and manures (Sun and Jaisi, 2018). Sun et al. (2017) reported *myo*-(1,3,4,5,6)-IP_5 and *myo*-(1,2,4,5,6)-IP_5 as intermediates in the minor pathways and major pathways, respectively, of *Aspergillus niger* phytase and acid phosphatase (potato) phytate degradation. The presence of *myo*-(1,2,3,4,6)-IP_5 could not be confirmed as NMR analyses on the compound itself exhibited a broad NMR signal (Fig. S7 in the Supplement). This is because in solutions with a pH of 9.5 or above, the 1-axial–5-equatorial and 5-axial–1-equatorial forms of *myo*-(1,2,3,4,6)-IP_5 are in a dynamic equilibrium, which can cause broadening (Volkmann et al., 2002). According to Turner and Richardson (2004) and Chung et al. (1999), the two identified *scyllo*-IP_4 peaks (signal pattern 2 : 2) can be attributed to the *scyllo*-(1,2,3,4)-IP_4 isomer. However, the two peaks of *scyllo*-IP_4 overlapped in the Cambisol and Gleysol with the peak at the furthest upfield chemical shift of *myo*-(1,2,4,5,6)-IP_5 at δ 3.25 ppm and with the peak at the furthest downfield chemical shift of *myo*-(1,3,4,5,6)-IP_5 at δ 4.12 ppm. Turner and Richardson (2004) reported NMR signals for two other *scyllo*-IP_4 isomers, which could not be tested for in this study due to the lack of available standards.

Whilst on average 48 % of the sharp peaks in the phosphomonoester region of soil extracts following hypobromite oxidation could be attributed to IP_6, IP_5 and *scyllo*-IP_4, the identities of many sharp peaks remain unknown. An unidentified peak at δ 4.33 ppm is present in all soil samples except in the Ferralsol, with concentrations of up to 10 mg P per kg soil (Cambisol). Other unidentified peaks at δ 3.49, 3.86, 4.20 and 3.91 ppm were detected in all soils, with concentrations ranging from 1 to 2 mg P per kg soil. Interestingly, two peaks upfield of *scyllo*-IP_6 became more prominent (at δ 3.08 and 3.05 ppm) following hypobromite oxidation, which was particularly the case in the Vertisol soil. The diversity of organic P species in the Vertisol soil appears to be much greater than previously reported (McLaren et al., 2014). We hypothesise that many of these unidentified peaks arise from other isomers of *myo*- and *scyllo*-IP_5, based on the higher abundance of their IP_6 counterparts.

The ratio of IP_6 to lower-order IP varied across soils, which ranged in decreasing order: Gleysol $\gg$ Cambisol > Vertisol > Ferralsol. McKercher and Anderson (1968a) found a higher ratio of IP_6 to IP_5 in some Scottish soils (ratio 1.8 to 4.6) compared to some Canadian soils (0.9 to 2.4). The authors attributed this difference to the greater stabilisation of IP_6 relative to lower esters in the Scottish soils, possibly due to climatic reasons or effects of different soil properties. In a subsequent study, McKercher and Anderson (1968b) observed increased IP contents with increasing total organic P content. Studies of organic P speciation along chronosequences found that *myo*-IP_6 concentrations declined in older soils (McDowell et al., 2007; Turner et al., 2007a, 2014). Similarly, Baker (1976) found that the $IP_6 + IP_5$ concentrations in the Franz Josef chronosequence increased until reaching 1000 years, followed by a rapid decline. In our soil samples, the highest IP_6-to-IP_5 ratio was found in the soil with the highest SOM content, suggesting a possible stabilisation of IP_6 due to association with SOM (Borie et al., 1989; Makarov et al., 1997). In contrast, the Ferralsol sample containing high amounts of Fe and Al showed the smallest IP_6-to-IP_5 ratio, even though IP_6 is known to strongly adsorb to sesquioxides (Anderson and Arlidge, 1962; Anderson et al., 1974). However, the production, input and mineralisation rates of IP_6 and IP_5 are not known for our soil samples. Further research is needed to understand the mechanisms controlling the flux of lower-order IP in soil.

In the Ferralsol and the Cambisol, there was an overall decrease in the concentration of IP_6 and IP_5 following hypobromite oxidation compared to the untreated extracts. Since the main cause of resistance of IP to hypobromite oxidation is that of steric hindrance, which generally decreases with a decreasing phosphorylation state and conformation of the phosphate groups (axial vs. equatorial), we assume that low recoveries of added *myo*-IP_6 are due to losses of precipitated P_{org} compounds during the precipitation and dissolution steps. This is supported by the decrease in the concentration of orthophosphate following hypobromite oxidation compared to untreated extracts. Therefore, quantities of IP as reported in the current study should be considered as conservative.

4.3 Structural composition of phosphomonoesters in hypobromite oxidised soil extracts

The NMR spectra on hypobromite oxidised soil extracts revealed the presence of sharp and broad signals in the phosphomonoester region. Transverse relaxation experiments revealed a rapid decay of the broad signal compared to the sharp peaks of IP_6, which support the hypothesis that the compounds causing the broad signal arise from P compounds other than IP. These findings are consistent with those of McLaren et al. (2019), who probed the structural composition of phosphomonoesters in untreated soil extracts. Overall, measured T_2 times in the current study on hypobromite oxidised extracts were markedly longer compared to those of untreated extracts reported in McLaren et al. (2019). This could be due to removal of other organic compounds by hypobromite oxidation in the matrix and therefore a decrease in the viscosity of the sample. This would result in an overall faster tumbling of the molecules and hence an increased T_2 relaxation time. As reported by McLaren et al. (2019), calculations of the broad signal's linewidth based on the T_2 times were considerably lower compared to those of the standard deconvolution fitting (SDF). When applying the same calculations to our samples, the linewidth of the broad signal at half height is on average 5.2 Hz based on the T_2 times. In contrast, the linewidths acquired from the SDF average 256.1 Hz. McLaren et al. (2019) suggested that the broad signal is itself comprised of more than one compound. Our re-

sults are consistent with this view, and therefore it is likely that the main cause of the broad signal is a diversity of P molecules of differing chemical environments within this region, rather than the slow tumbling of just one macromolecule. Nebbioso and Piccolo (2011) reported that high-molecular-weight material of organic matter in soil is an association of smaller organic molecules. We suggest that these associations would still cause a broad signal in the phosphomonoester region of soil extracts and could be a reason that some organic molecules containing P are protected from hypobromite oxidation.

Since a portion of the broad signal is resistant to hypobromite oxidation, this suggests the organic P is complex and in the form of polymeric structures. The chemical resistance of the broad signal to hypobromite oxidation may also indicate a high stability in soil (Jarosch et al., 2015). Annaheim et al. (2015) found that concentrations of the broad signal remained unchanged across three different organic fertiliser strategies after 62 years of cropping. In contrast, the organic P compounds annually added with the fertilisers were completely transformed or lost in the slightly acidic topsoil of the field trial. The large proportion of the broad signal in the total organic P pool demonstrates its importance in the soil P cycle.

Unexpectedly, the transverse relaxation times of orthophosphate were shorter than those of the broad signal. This was similarly the case in an untreated NaOH-EDTA extract of a forest soil with the same origin as the Cambisol as reported in McLaren et al. (2019). The authors hypothesised that this might be due to the sample matrix (i.e. high concentration of metals and organic matter). Whilst these factors are likely to affect T_2 times, they do not appear to be the main cause as the hypobromite oxidised extracts in the current study contained low concentrations of organic matter and metals as a consequence of the isolation procedure. The fast decay of orthophosphate was found across all four soil extracts with a diverse array of organic P concentrations and compositions of organic P in the phosphomonoester region. Therefore, another possible explanation could be a matrix effect or an association with large organic P compounds causing the broad signal (McLaren et al., 2019). It is known that dynamic intramolecular processes such as ring inversion and intermolecular processes such as binding of small-molecule ligands to macromolecules can cause a broadening or a doubling of resonances (Claridge, 2016). When the smaller molecule is bound to the larger molecule, it experiences slower tumbling in the solution and hence a shorter T_2 time. It is possible that a chemical exchange of the orthophosphate with a compound in the matrix or an organic P molecule could result in the short T_2 time of the orthophosphate peak. We carried out a T_2 experiment on a pure solution of monopotassium phosphate (described in the Supplement), in which the matrix effects should be considerably reduced compared to the soil extracts. We found that the T_2 time of orthophosphate (203 ms) in the pure solution was considerably longer than that reported in soil extracts following hypobromite oxidation.

5 Conclusions

Inositol phosphates are an important pool of organic P in soil, but information on the mechanisms controlling their flux in soil remains limited due in part to an inability to detect them using solution ^{31}P NMR spectroscopy. For the first time, we identified six different lower-order IPs in the solution ^{31}P NMR spectra on soil extracts. Solution ^{31}P NMR spectra on hypobromite oxidised extracts revealed the presence of up to 70 sharp peaks, of which about 50 % could be identified. Our results indicate that a majority of the sharp peaks in solution ^{31}P NMR soil spectra were resistant to hypobromite oxidation and therefore suggest the presence of diverse IPs. Our study highlights the great diversity and abundance of IPs in soils and therefore their importance in terrestrial P cycles. Further research on the mechanisms and processes involved in the cycling of this wide variety of IPs in soil will have implications for our understanding of organic P turnover as well as plant availability and possibly help improve fertiliser strategies in agricultural systems.

Furthermore, we provide new insight into the large pool of phosphomonoesters represented by the broad signal, of which a considerable portion was resistant to hypobromite oxidation. Further research is needed to understand the chemical composition of the broad signal and the mechanisms controlling its flux in terrestrial ecosystems.

Data availability. All data presented in this study and the Supplement are also available by request from the corresponding author.

Supplement. The supplement related to this article is available online at: https://doi.org/10.5194/bg-17-5079-2020-supplement.

Author contributions. The experimental design was planned by JER, TIM, DZ, RV and EF. The experiments were carried out by JER under the supervision of TIM, DZ and RV. RV provided the MATLAB code for the standard deconvolution fitting of the NMR spectra. The data were processed, analysed and interpreted by JER with support from TIM, DZ and RV. JER prepared the manuscript with contributions from all co-authors.

Competing interests. The authors declare that they have no conflict of interest.

Acknowledgements. The authors are grateful to Laurie Paule Schönholzer, Federica Tamburini, Björn Studer, Monika Macsai and Charles Brearley for technical support.

Furthermore, the authors thank Astrid Oberson, David Lester, Chiara Pistocchi and Gregor Meyer for providing soil samples. This study would not have been possible without the IP standards originating from the late Dennis Cosgrove collection and Max Tate collection, which we highly appreciate.

Financial support. This research has been supported by the Swiss National Science Foundation (grant no. 200021_169256).

Review statement. This paper was edited by Sébastien Fontaine and reviewed by three anonymous referees.

References

Almeida, D. S., Menezes-Blackburn, D., Turner, B. L., Wearing, C., Haygarth, P. M., and Rosolem, C. A.: Urochloa ruziziensis cover crop increases the cycling of soil inositol phosphates, Biol. Fert. Soils, 54, 935–947, https://doi.org/10.1007/s00374-018-1316-3, 2018.

Anderson, G.: Paper chromatography of inositol phosphates, Nature, 175, 863–864, https://doi.org/10.1038/175863b0, 1955.

Anderson, G. and Arlidge, E. Z.: The adsorption of inositol phosphates and glycerophosphate by soil clays, clay minerals, and hydrated sesquioxides in acid media, J. Soil Sci., 13, 216–224, https://doi.org/10.1111/j.1365-2389.1962.tb00699.x, 1962.

Anderson, G. and Malcolm, R. E.: The nature of alkali-soluble soil organic phosphates., J. Soil Sci., 25, 282–297, https://doi.org/10.1111/j.1365-2389.1974.tb01124.x, 1974.

Anderson, G., Williams, E. G., and Moir, J. O.: A comparison of the sorption of inorganic orthophosphate and inositol hexaphosphate by six acid soils, J. Soil Sci., 25, 51–62, https://doi.org/10.1111/j.1365-2389.1974.tb01102.x, 1974.

Angyal, S. J.: Cyclitols, in: Comprehensive Biochemistry, edited by: Florkin, M. and Stotz, E. H., Elsevier, chap. VIII, 53 Vanderbilt Avenue, New York 17, NY, 297–303, 1963.

Annaheim, K. E., Doolette, A. L., Smernik, R. J., Mayer, J., Oberson, A., Frossard, E., and Bünemann, E. K.: Long-term addition of organic fertilizers has little effect on soil organic phosphorus as characterized by ^{31}P NMR spectroscopy and enzyme additions, Geoderma, 257–258, 67–77, https://doi.org/10.1016/j.geoderma.2015.01.014, 2015.

Baker, R. T.: Changes in the chemical nature of soil organic phosphate during pedogenesis., J. Soil Sci., 27, 504–512, https://doi.org/10.1111/j.1365-2389.1976.tb02020.x, 1976.

Borie, F., Zunino, H., and Martínez, L.: Macromolecule associations and inositol phosphates in some chilean volcanic soils of temperate regions, Commun. Soil Sci. Plan., 20, 1881–1894, https://doi.org/10.1080/00103628909368190, 1989.

Bühler, S., Oberson, A., Sinaj, S., Friesen, D. K., and Frossard, E.: Isotope methods for assessing plant available phosphorus in acid tropical soils, Eur. J. Soil Sci., 54, 605–616, https://doi.org/10.1046/j.1365-2389.2003.00542.x, 2003.

Bünemann, E. K., Smernik, R. J., Marschner, P., and McNeill, A. M.: Microbial synthesis of organic and condensed forms of phosphorus in acid and calcareous soils, Soil Biol. Biochem., 40, 932–946, https://doi.org/10.1016/j.soilbio.2007.11.012, 2008.

Bünemann, E. K., Augstburger, S., and Frossard, E.: Dominance of either physicochemical or biological phosphorus cycling processes in temperate forest soils of contrasting phosphate availability, Soil Biol. Biochem., 101, 85–95, https://doi.org/10.1016/j.soilbio.2016.07.005, 2016.

Cade-Menun, B. J.: Improved peak identification in ^{31}P-NMR spectra of environmental samples with a standardized method and peak library, Geoderma, 257–258, 102–114, https://doi.org/10.1016/j.geoderma.2014.12.016, 2015.

Cade-Menun, B. and Liu, C. W.: Solution phosphorus-31 nuclear magnetic resonance spectroscopy of soils from 2005 to 2013: a review of sample preparation and experimental parameters, Soil Sci. Soc. Am. J., 78, 19–37, https://doi.org/10.2136/sssaj2013.05.0187dgs, 2014.

Cade-Menun, B. J. and Preston, C. M.: A comparison of soil extraction procedures for ^{31}P NMR spectroscopy, Soil Sci., 161, 770–785, 1996.

Cade-Menun, B. J., Liu, C. W., Nunlist, R., and McColl, J. G.: Soil and litter phosphorus-31 nuclear magnetic resonance spectroscopy, J. Environ. Qual., 31, 457–465, https://doi.org/10.2134/jeq2002.4570, 2002.

Celi, L. and Barberis, E.: Abiotic reactions of inositol phosphates in soil, in: Inositol phosphates: linking agriculture and the environment, edited by: Turner, B. L., Richardson, A. E., and Mullaney, E. J., CABI, Wallingford, 207–220, 2007.

Chung, S.-K., Kwon, Y.-U., Chang, Y.-T., Sohn, K.-H., Shin, J.-H., Park, K.-H., Hong, B.-J., and Chung, I.-H.: Synthesis of all possible regioisomers of *scyllo*-Inositol phosphate, Bioorgan. Med. Chem., 7, 2577–2589, https://doi.org/10.1016/S0968-0896(99)00183-2, 1999.

Claridge, T. D. W.: Introducing High-Resolution NMR, in: High-Resolution NMR techniques in organic chemistry, 3rd edn., edited by: Claridge, T. D. W., Elsevier, Boston, chap. 2, 11–59, 2016.

Cosgrove, D.: The chemical nature of soil organic phosphorus. I. Inositol phosphates, Soil Res., 1, 203–214, https://doi.org/10.1071/SR9630203, 1963.

Cosgrove, D. J. and Irving, G. C. J.: Inositol phosphates: their chemistry, biochemistry and physiology, Studies in organic chemistr, Elsevier, Amsterdam, 1980.

Doolette, A. L. and Smernik, R. J.: Phosphorus speciation of dormant grapevine (Vitis vinifera L.) canes in the Barossa Valley, South Australia, Aust. J. Grape Wine R., 22, 462–468, https://doi.org/10.1111/ajgw.12234, 2016.

Doolette, A. L. and Smernik, R. J.: Facile decomposition of phytate in the solid-state: kinetics and decomposition pathways, Phosphorus Sulfur, 193, 192–199, https://doi.org/10.1080/10426507.2017.1416614, 2018.

Doolette, A. L., Smernik, R. J., and Dougherty, W. J.: Spiking improved solution phosphorus-31 nuclear magnetic resonance identification of soil phosphorus compounds, Soil Sci. Soc. Am. J., 73, 919–927, https://doi.org/10.2136/sssaj2008.0192, 2009.

Doolette, A. L., Smernik, R. J., and Dougherty, W. J.: A quantitative assessment of phosphorus forms in some Australian soils, Soil Res., 49, 152–165, https://doi.org/10.1071/SR10092, 2011a.

Doolette, A. L., Smernik, R. J., and Dougherty, W. J.: Overestimation of the importance of phytate in NaOH–EDTA soil extracts as assessed by 31P NMR analyses, Org. Geochem., 42, 955–964, https://doi.org/10.1016/j.orggeochem.2011.04.004, 2011b.

Dougherty, W. J., Smernik, R. J., and Chittleborough, D. J.: Application of spin counting to the solid-state ^{31}P NMR analysis of pasture soils with varying phosphorus content, Soil Sci. Soc. Am. J., 69, 2058–2070, 10.2136/sssaj2005.0017, 2005.

Dougherty, W. J., Smernik, R. J., Bünemann, E. K., and Chittleborough, D. J.: On the use of hydrofluoric acid pretreatment of soils for phosphorus-31 nuclear magnetic resonance analyses, Soil Sci. Soc. Am. J., 71, 1111–1118, https://doi.org/10.2136/sssaj2006.0300, 2007.

Dyer, W. J. and Wrenshall, C. L.: Organic phosphorus in soils: III. The decomposition of some organic phosphorus compounds in soil cultures, Soil Sci., 51, 323–329, 1941.

FAO and Group, I. W.: World reference base for soil resources 2014, World soil resources reports, Food and Agriculture Organization of the United Nations FAO, Rome, 2014.

Fatiadi, A. J.: Bromine oxidation of inositols for preparation of inosose phenylhydrazones and phenylosazones, Carbohyd. Res., 8, 135–147, https://doi.org/10.1016/S0008-6215(00)80149-4, 1968.

Golovan, S. P., Meidinger, R. G., Ajakaiye, A., Cottrill, M., Wiederkehr, M. Z., Barney, D. J., Plante, C., Pollard, J. W., Fan, M. Z., Hayes, M. A., Laursen, J., Hjorth, J. P., Hacker, R. R., Phillips, J. P., and Forsberg, C. W.: Pigs expressing salivary phytase produce low-phosphorus manure, Nat. Biotechnol., 19, 741–745, https://doi.org/10.1038/90788, 2001.

Goring, C. A. I. and Bartholomew, W. V.: Microbial products and soil organic matter: III. Adsorption of carbohydrate phosphates by clays, Soil Sci. Soc. Am. J., 15, 189–194, https://doi.org/10.2136/sssaj1951.036159950015000C0043x, 1951.

Halstead, R. L. and Anderson, G.: Chromatographic fractionation of organic phosphates from alkali, acid, and aqueous acetylacetone extracts of soils, Can. J. Soil Sci., 50, 111–119, https://doi.org/10.4141/cjss70-018, 1970.

Hochberg, Y. and Tamhane, A. C.: Multiple comparison procedures, Wiley series in probability and mathematical statistics. Applied probability and statistics, Wiley, New York, 1987.

Irvine, R. F. and Schell, M. J.: Back in the water: the return of the inositol phosphates, Nat. Rev. Mol. Cell Bio., 2, 327, https://doi.org/10.1038/35073015, 2001.

Irving, G. C. J. and Cosgrove, D. J.: The use of hypobromite oxidation to evaluate two current methods for the estimation of inositol polyphosphates in alkaline extracts of soils, Commun. Soil Sci. Plan., 12, 495–509, https://doi.org/10.1080/00103628109367169, 1981.

Irving, G. C. J. and Cosgrove, D. J.: The use of gasliquid chromatography to determine the proportions of inositol isomers present as pentakis and hexakisphosphates in alkaline extracts of soils, Commun. Soil Sci. Plan., 13, 957–967, https://doi.org/10.1080/00103628209367324, 1982.

Jarosch, K. A., Doolette, A. L., Smernik, R. J., Tamburini, F., Frossard, E., and Bünemann, E. K.: Characterisation of soil organic phosphorus in NaOH-EDTA extracts: a comparison of ^{31}P NMR spectroscopy and enzyme addition assays, Soil Biol. Biochem., 91, 298–309, https://doi.org/10.1016/j.soilbio.2015.09.010, 2015.

Lang, F., Krüger, J., Amelung, W., Willbold, S., Frossard, E., Bünemann, E. K., Bauhus, J., Nitschke, R., Kandeler, E., Marhan, S., Schulz, S., Bergkemper, F., Schloter, M., Luster, J., Guggisberg, F., Kaiser, K., Mikutta, R., Guggenberger, G., Polle, A., Pena, R., Prietzel, J., Rodionov, A., Talkner, U., Meesenburg, H., von Wilpert, K., Hölscher, A., Dietrich, H. P., and Chmara, I.: Soil phosphorus supply controls P nutrition strategies of beech forest ecosystems in Central Europe, Biogeochemistry, 136, 5–29, https://doi.org/10.1007/s10533-017-0375-0, 2017.

L'Annunziata, M. F.: The origin and transformations of the soil inositol phosphate isomers, Soil Sci. Soc. Am. J., 39, 377–379, https://doi.org/10.2136/sssaj1975.03615995003900020041x, 1975.

Leytem, A. B. and Maguire, R. O.: Environmental implications of inositol phosphates in animal manures, in: Inositol phosphates: linking agriculture and the environment, edited by: Turner, B. L., Richardson, A. E., and Mullaney, E. J., CABI, Wallingford, 150–168, 2007.

Leytem, A. B., Turner, B. L., and Thacker, P. A.: Phosphorus composition of manure from swine fed low-phytate grains, J. Environ. Qual., 33, 2380–2383, https://doi.org/10.2134/jeq2004.2380, 2004.

Li, M., Cozzolino, V., Mazzei, P., Drosos, M., Monda, H., Hu, Z., and Piccolo, A.: Effects of microbial bioeffectors and P amendements on P forms in a maize cropped soil as evaluated by ^{31}P–NMR spectroscopy, Plant Soil, 427, 87–104, https://doi.org/10.1007/s11104-017-3405-8, 2018.

Makarov, M. I., Malysheva, T. I., Haumaier, L., Alt, H. G., and Zech, W.: The forms of phosphorus in humic and fulvic acids of a toposequence of alpine soils in the northern Caucasus, Geoderma, 80, 61–73, https://doi.org/10.1016/S0016-7061(97)00049-9, 1997.

McDowell, R. W. and Stewart, I.: The phosphorus composition of contrasting soils in pastoral, native and forest management in Otago, New Zealand: Sequential extraction and ^{31}P NMR, Geoderma, 130, 176–189, https://doi.org/10.1016/j.geoderma.2005.01.020, 2006.

McDowell, R. W., Cade-Menun, B., and Stewart, I.: Organic phosphorus speciation and pedogenesis: analysis by solution ^{31}P nuclear magnetic resonance spectroscopy, Eur. J. Soil Sci., 58, 1348–1357, https://doi.org/10.1111/j.1365-2389.2007.00933.x, 2007.

McKercher, R. B. and Anderson, G.: Characterization of the inositol penta- and hexaphosphate fractions of a number of Canadian and Scottish soils, J. Soil Sci., 19, 302–310, https://doi.org/10.1111/j.1365-2389.1968.tb01542.x, 1968a.

McKercher, R. B. and Anderson, G.: Content of inositol penta- and hexaphosphates in some Canadian soils, J. Soil Sci., 19, 47–55, https://doi.org/10.1111/j.1365-2389.1968.tb01519.x, 1968b.

McKercher, R. B. and Anderson, G.: Organic phosphate sorption by neutral and basic soils, Commun. Soil Sci. Plan., 20, 723–732, https://doi.org/10.1080/00103628909368112, 1989.

McLaren, T. I., Smernik, R. J., Guppy, C. N., Bell, M. J., and Tighe, M. K.: The organic P composition of vertisols as determined by ^{31}P NMR spectroscopy, Soil Sci. Soc. Am. J., 78, 1893–1902, https://doi.org/10.2136/sssaj2014.04.0139, 2014.

McLaren, T. I., Simpson, R. J., McLaughlin, M. J., Smernik, R. J., McBeath, T. M., Guppy, C. N., and Richardson, A. E.: An assessment of various measures of soil phosphorus and the net accumulation of phosphorus in fertilized soils under pasture, J. Plant Nutr. Soil Sci., 178, 543–554, https://doi.org/10.1002/jpln.201400657, 2015a.

McLaren, T. I., Smernik, R. J., McLaughlin, M. J., McBeath, T. M., Kirby, J. K., Simpson, R. J., Guppy, C. N., Doolette, A. L., and Richardson, A. E.: Complex forms of soil organic phosphorus–A major component of soil phosphorus, Environ. Sci. Technol., 49, 13238–13245, https://doi.org/10.1021/acs.est.5b02948, 2015b.

McLaren, T. I., Verel, R., and Frossard, E.: The structural composition of soil phosphomonoesters as determined by solution ^{31}P NMR spectroscopy and transverse relaxation (T_2) experiments, Geoderma, 345, 31–37, https://doi.org/10.1016/j.geoderma.2019.03.015, 2019.

Meiboom, S. and Gill, D.: Modified spinecho method for measuring nuclear relaxation times, Rev. Sci. Instrum., 29, 688–691, https://doi.org/10.1063/1.1716296, 1958.

Milliken, G. A. and Johnson, D. E.: Analysis of messy data. Volume 1: designed experiments, 2nd edn., CRC Press, Boca Raton, Florida, 2009.

Nebbioso, A. and Piccolo, A.: Basis of a Humeomics science: chemical fractionation and molecular characterization of humic biosuprastructures, Biomacromolecules, 12, 1187–1199, https://doi.org/10.1021/bm101488e, 2011.

Newman, R. H. and Tate, K. R.: Soil phosphorus characterisation by ^{31}P nuclear magnetic resonance, Commun. Soil Sci. Plan., 11, 835–842, https://doi.org/10.1080/00103628009367083, 1980.

Ognalaga, M., Frossard, E., and Thomas, F.: Glucose-1-phosphate and *myo*-inositol hexaphosphate adsorption mechanisms on goethite, Soil Sci. Soc. Am. J., 58, 332–337, https://doi.org/10.2136/sssaj1994.03615995005800020011x, 1994.

Ohno, T. and Zibilske, L. M.: Determination of low concentrations of phosphorus in soil extracts using malachite green, Soil Sci. Soc. Am. J., 55, 892–895, https://doi.org/10.2136/sssaj1991.03615995005500030046x, 1991.

Reusser, J. E., Verel, R., Frossard, E., and McLaren, T. I.: Quantitative measures of *myo*-IP_6 in soil using solution ^{31}P NMR spectroscopy and spectral deconvolution fitting including a broad signal, Environ. Sci. – Proc. Imp., 22, 1084–1094, https://doi.org/10.1039/C9EM00485H, 2020.

Riley, A. M., Trusselle, M., Kuad, P., Borkovec, M., Cho, J., Choi, J. H., Qian, X., Shears, S. B., Spiess, B., and Potter, B. V. L.: *scyllo* Inositol pentakisphosphate as an analogue of *myo* inositol 1,3,4,5,6: Chemical synthesis, physicochemistry and biological applications, ChemBioChem, 7, 1114–1122, https://doi.org/10.1002/cbic.200600037, 2006.

Sharma, V. K.: Oxidation of amino acids, peptides, and proteins: kinetics and mechanism, Wiley series of reactive intermediates in chemistry and biology, Wiley, Hoboken, 2013.

Smith, D. H. and Clark, F. E.: Anion-exchange chromatography of inositol phosphates from soil, Soil Sci., 72, 353–360, 1951.

Spain, A. V., Tibbett, M., Ridd, M., and McLaren, T. I.: Phosphorus dynamics in a tropical forest soil restored after strip mining, Plant Soil, 427, 105–123, https://doi.org/10.1007/s11104-018-3668-8, 2018.

Stephens, L. R. and Irvine, R. F.: Stepwise phosphorylation of *myo*-inositol leading to *myo*-inositol hexakisphosphate in Dictyostelium, Nature, 346, 580–583, https://doi.org/10.1038/346580a0, 1990.

Strickland, K. P.: The chemistry of phospholipids, in: Form and Function of Phospholipids, 2nd edn., edited by: Ansell, G. B., Hawthorne, J. N., and Dawson, R. M. C., Elsevier Scientific Publ. Company, Amsterdam, the Netherlands, 1973.

Sun, M. and Jaisi, D. P.: Distribution of inositol phosphates in animal feed grains and excreta: distinctions among isomers and phosphate oxygen isotope compositions, Plant Soil, 430, 291–305, https://doi.org/10.1007/s11104-018-3723-5, 2018.

Sun, M., Alikhani, J., Massoudieh, A., Greiner, R., and Jaisi, D. P.: Phytate degradation by different phosphohydrolase enzymes: contrasting kinetics, decay rates, pathways, and isotope effects, Soil Sci. Soc. Am. J., 81, 61–75, https://doi.org/10.2136/sssaj2016.07.0219, 2017.

Suzumura, M. and Kamatani, A.: Isolation and determination of inositol hexaphosphate in sediments from Tokyo Bay, Geochim. Cosmochim. Ac., 57, 2197–2202, https://doi.org/10.1016/0016-7037(93)90561-A, 1993.

Turner, B. L.: Inositol phosphates in soil: Amounts, forms and significance of the phosphorylated inositol stereoisomers., in: Inositol phosphates: Linking agriculture and the environment., edited by: Turner, B. L., Richardson, A. E., and Mullaney, E. J., CAB International, Wallingford, Oxfordshire, UK, 186–206, 2007.

Turner, B. L.: Soil organic phosphorus in tropical forests: an assessment of the NaOH–EDTA extraction procedure for quantitative analysis by solution ^{31}P NMR spectroscopy, Eur. J. Soil Sci., 59, 453–466, https://doi.org/10.1111/j.1365-2389.2007.00994.x, 2008.

Turner, B. L.: Isolation of inositol hexakisphosphate from soils by alkaline extraction and hypobromite oxidation, in: Inositol Phosphates: Methods and Protocols, edited by: Miller, G. J., Springer US, New York, NY, 39–46, 2020.

Turner, B. L. and Richardson, A. E.: Identification of *scyllo*-inositol phosphates in soil by solution phosphorus-31 nuclear magnetic resonance spectroscopy, Soil Sci. Soc. Am. J., 68, 802–808, https://doi.org/10.2136/sssaj2004.8020, 2004.

Turner, B. L., Papházy, M. J., Haygarth, P. M., and McKelvie, I. D.: Inositol phosphates in the environment, Philos. T. Roy. Soc. B, 357, 449–469, https://doi.org/10.1098/rstb.2001.0837, 2002.

Turner, B. L., Condron, L. M., Richardson, S. J., Peltzer, D. A., and Allison, V. J.: Soil organic phosphorus transformations during pedogenesis, Ecosystems, 10, 1166–1181, https://doi.org/10.1007/s10021-007-9086-z, 2007a.

Turner, B. L., Richardson, A. E., and Mullaney, E. J.: Inositol phosphates: linking agriculture and the environment, CABI, Wallingford, xi + 288 pp., 2007b.

Turner, B. L., Cheesman, A. W., Godage, H. Y., Riley, A. M., and Potter, B. V.: Determination of *neo*- and D-*chiro*-inositol hexakisphosphate in soils by solution ^{31}P NMR spectroscopy, Environ. Sci. Technol., 46, 4994–5002, https://doi.org/10.1021/es204446z, 2012.

Turner, B. L., Wells, A., and Condron, L. M.: Soil organic phosphorus transformations along a coastal dune chronosequence under New Zealand temperate rain forest, Biogeochemistry, 121, 595–611, https://doi.org/10.1007/s10533-014-0025-8, 2014.

Vestergren, J., Vincent, A. G., Jansson, M., Persson, P., Ilstedt, U., Gröbner, G., Giesler, R., and Schleucher, J.: High-resolution characterization of organic phosphorus in soil extracts using 2D ^{1}H–^{31}P NMR correlation spectroscopy, Environ. Sci. Technol., 46, 3950–3956, https://doi.org/10.1021/es204016h, 2012.

Vincent, A. G., Vestergren, J., Gröbner, G., Persson, P., Schleucher, J., and Giesler, R.: Soil organic phosphorus transformations

in a boreal forest chronosequence, Plant Soil, 367, 149–162, https://doi.org/10.1007/s11104-013-1731-z, 2013.

Vold, R. L., Waugh, J. S., Klein, M. P., and Phelps, D. E.: Measurement of spin relaxation in complex systems, J. Chem. Phys., 48, 3831–3832, https://doi.org/10.1063/1.1669699, 1968.

Volkmann, C. J., Chateauneuf, G. M., Pradhan, J., Bauman, A. T., Brown, R. E., and Murthy, P. P. N.: Conformational flexibility of inositol phosphates: influence of structural characteristics, Tetrahedron Lett., 43, 4853–4856, https://doi.org/10.1016/S0040-4039(02)00875-4, 2002.

Zhang, X., Li, Z., Yang, H., Liu, D., Cai, G., Li, G., Mo, J., Wang, D., Zhong, C., Wang, H., Sun, Y., Shi, J., Zheng, E., Meng, F., Zhang, M., He, X., Zhou, R., Zhang, J., Huang, M., Zhang, R., Li, N., Fan, M., Yang, J., and Wu, Z.: Novel transgenic pigs with enhanced growth and reduced environmental impact, eLife, 7, e34286, https://doi.org/10.7554/eLife.34286, 2018.